Geological and mechanical rock mass conditions for TBM performance prediction. The case of “La Maddalena” exploratory tunnel, Chiomonte (Italy)

GEOLOGICAL AND MECHANICAL ROCK MASS CONDITIONS FOR TBM PERFORMANCE PREDICTION. THE CASE OF "LA MADDALENA" EXPLORATORY TUNNEL. CHIOMONTE, ITALY

Armetti Giacomo[1], Migliazza Maria Rita[2], Federica Ferrari[3], Berti Andrea[4], Padovese Paolo[4]

[1] Università degli Studi di Milano, Dipartimento di Scienze della Terra "A. Desio"

[2] Politecnico di Torino, DISEG

[3] Eni, Exploration and Production – Operational Geology

[4] CMC Cooperativa Muratori e Cementisti di Ravenna

Abstract:

The Tunnel Boring Machine (TBM) performance prediction is fundamental in order to select the most effective tunnel construction methods and to estimate the condition of excavation in terms of time and economic costs of the infrastructure. Many researchers have developed several empirical and theoretical models, the most of which based on the comparison between geological-geotechnical rock masses characteristics and TBM data. However, these models are specific-site and hardly applicable to different context. The aim of this work is to carried out easy models utilizable during early stage of tunnel planning and realization; for this purpose singular rock mass parameters (UCS, quartz content, spacing between fractures, etc.) have been related to TBM performance indices, as ROP (Rate of Penetration) and FPI (Field Penetration Index). In particular this study focuses on "La Maddalena" exploratory tunnel (Tunnel Euroalpin Lyon-Turin), situated in northern Italy, where geological, geotechnical and TBM performance data have been continuously collected during tunnel construction.

Key words

Open gripper main beam Tunnel Boring Machine

TBM performance prediction

Penetration Rate

Field Penetration Index

Rock mass characterization

1. Introduction

The planning of tunnel projects and the consequent selection of construction methods require the effective prediction of TBM performance in order to make tunneling more effective and cheaper than traditional drill and blast construction method, guaranteeing concurrently the same construction level of safety. During the last decades many researchers (Barton, 2000; Blindheim, 1979; Bilgin et al., 2013; Gong and Zhao, 2009; Hamidi et al., 2010; Hassanpour et al., 2011; Macias, 2014; Nelson and O'Rourke, 1983; Ozdemir, 1977; Rostami and Ozdemir, 1993; Sapigni et al., 2002; Tarkoy, 1975; Yagiz, 2002, 2006, 2008) have developed several methods that allow to estimate the TBM performance, by analyzing the interaction between the rock mass features and the operating characteristics of the TBM.

The TBM performance predictive models are based on two different approaches, the physical-mathematical approach and the empirical one.

The physical-mathematical ones are based on the breakage mechanism analysis and study the cutting forces acting on cutters in order to define a force equilibrium relation (Crow, 1975; Ozdemir et al., 1978; Roxborough and Phillips, 1975; Sanio, 1985; Sato et al., 1991; Snowdon et al., 1982). Nevertheless, these models are difficult to apply, because they require several laboratory tests, which sometimes do not represent the real rock masses behavior during tunnels excavation.

The empirical models are based on measured data of intact rock and rock mass features (i.e., UCS, quartz content, fracturing degree, etc.), and TBM performance parameters collected continuously

during the entire excavation phases. Afterwards, correlations between the measured geological/geomechanical parameters and TBM data are defined. In general, the empirical models offer the greatest correspondence with the reality. Nevertheless, they are limited by the fact that the proposed correlations are site-specific, being strongly related to the analyzed case study, and hardly applicable to different geological contexts (Brino et al., 2015). In some studies, the correlations take into account a single intact rock parameter, such as the Uniaxial Compressive Strength (UCS; Farmer and Glossop, 1980; Graham, 1976; Hughes, 1986), or rock matrix index, such as the Drilling Rate Index (DRI), punch penetration, Taber abrasion, Brazilian tensile strength, Shore harness and point load index (Bamford, 1984; Blindheim, 1979; Dollinger et al., 1998; Nelson et al., 1983, 1985; Tarkoy, 1973; Wijk, 1992). The chosen parameter was then related to a TBM performance index. Some models are instead based on multiple factors involving both intact rock-rock mass parameters and machine ones (Bruland, 1998; Grima et al., Nelson et al., 1999; 2000; Sundin and Wanstedt, 1994; Yagiz, 2008; Zhao et al., 2007). Multifactor models are difficult to be applied because both they are specific-site developed and several rock parameters have to be investigated. At the Colorado School of Mining (CSM; Rostami, 1997; Rostami and Ozdemir, 1993) a prediction model has been developed starting from a force equilibrium approach based on cutter geometry and mechanical properties of intact rock. Yagiz (2002) and Remezanzadeh et al. (2008) modified CSM model in order to include rock mass properties in the calculations, as UCS and tensile strength of rock.

Some models aim to correlate rock mass classifications with TBM performance (Innaurato et al., 1991; McFeat-Smith, 1999; Ribacchi and Fazio, 2005; Sapigni et al., 2002; Sundaram et al., 1998), such as Rock Structure Rating (RSR, Wickham et al., 1972), Rock Mass Rating (RMR, Bieniawski, 1989), Rock Mass Quality Index (Q, Barton et al., 1974) and Geological Strength Index (GSI, Hoek, 1994; Marinos and Hoek, 2000). The empirical models most widely used nowadays are the

Norwegian University of Science and Technology method (NTNU, Bruland, 1998) and Q_{TBM} system (Barton, 2000). The NTNU is based on the relationship between the geological, structural and geotechnical features of rock masses and the measured TBM performance.

The Q_{TBM} method is based on Q-system with the addition of some parameters as the quartz content, cutter life index and the stress on tunnel face. By the value obtained it is possible to estimate the performances of TBM both in terms of Penetration Rate, Advance Rate and Field Penetration Index. The table below (Table 1) summarizes the most adopted predictive methods.

Furthermore the gathering of rock mass data is strongly affected by the type of TBM used for tunneling: an open gripper machine useable in hard rock allows a continuous collection of rock mass data, while the use of a single or double shield TBM with the lining segments assembled directly behind the shield itself, impedes a direct survey of the rock wall.

The paper aims to develop a TBM performance predictive model based on the comparison between the geological and geomechanical rock mass features and the TBM performance data collected during the excavation of “La Maddalena” exploratory tunnel. As following more detailed described, the tunnel has been realized by the use of an open gripper TBM, allowing the authors to continuously collect a big amount of geomechanical rock mass data. For this purpose a tract of tunnel 2000 m long was investigated.

2. Description of the analyzed tunnel project

The exploratory tunnel named “La Maddalena” is located in Susa Valley, Western Alps, North Italy, (Figure 1) and has a length of 7500 m and a diameter of 6 m, its orientation was decided during design phase and it is 307° (from North) at the beginning of excavation, then it increases up to 330°. The tunnel is one of the infrastructures connected to the realization of the high-speed rail that will link Lyon (France) to Turin (Italy). This is currently one of the most important European

projects, because it represents the fundamental joint of the railway line that aims to connect Seville (Spain) to Budapest (Hungary). The excavation is realized by means of an open gripper main beam TBM produced by the Robbin's Company, the main TBM features are summarized in table 2. The encountered rock mass has a global good quality, which gives acceptable safety conditions in underground, so that reinforcement and/or support elements are not necessary, being the cavity self-sustaining. Rock bolts, steel ribs and sprayed concrete are utilized only in case of intense fracturing (i.e., during faults or cataclastic zones crossing), or localized zones with poor rock mass features. In most of the length, cavity walls are without support elements and without shotcrete, hence tunnel walls are observable (in accordance with open TBM type). The tunnel depth ranges between 80 and 1000 m from the surface.

2.1 Regional geological setting

La Maddalena tunnel is excavated in the Ambin Massif, which is part of the Gran San Bernardo Nappe that structurally pertains to the middle Pennidic Domain (Figure 1). The Ambin Massif outcrops at the border between Italy and France, and forms a large antiform. It emerges in correspondence of a wide axial culmination under more tectonics elements belonging to Piedmontese nappe. Argand et al. (1911) joined the Massif to the upper Pennidic Nappe of Dora Maira, based on lithological evidences; afterwards, Staub (1937) and Ellenberger (1958), recognized that the Ambin Massif belongs to Brianconaise zone, in accordance with the Mesozoic cover features. By observing the litho-stratigraphic affinities, the Massif is correlated with Pontis nappe (Thelin et al., 1990) and with Chasseforet Massif (Desmons and Mercier, 1993). The tectono-stratigraphic unit of Ambin, outcropping between Chiomonte and Oulx, is composed by a pre-Triassic crystalline basement on which limited Mesozoic meta-sediments rest. The basement is divided into a base complex (named Clarea complex) and an upper one (Ambin complex). The former is characterized by poly-metamorphic schists with relict of pre-Alpine metamorphism,

while the latter is mainly composed by meta-volcanic rocks (Permian). The dividing horizon between the two units is in the order of tens of meters in thickness and consists of meta-conglomerates with quartz pebbles principally. The Ambin Massif Mesozoic cover, which is poorly conserved on its South side, is characterized by a carbonate sequence 20 m thick.

In the studied area, stress field is extensional type and shows two extensional processes. The first phase is considered a lateral extrusion of the inner Western Alpine Arc, the second one is due to body forces in the root of the belt and gravitational re-equilibration (Sue et al., 2007).

The area is affected by three main fault systems: the “Mompantero – Colle delle Finestre” the “Medium Susa Valley – Upper Chisone Valley” and “Sangone” shear zones.

The “Mompantero – Colle delle Finestre” fault system is a relevant structure with mean direction NNE-SSW, which is probably related to “Cenischia-Nizza line” (Casati and Giovacchini, 1977). This system has a mean direction of N20° and outcrops in the upper sector of Susa Valley and Mourienne, where there are N-S faults with reject evaluated in the order of kilometers. This system corresponds to the normal fault system of Modane – Termignon – Ruisseau de Chaviere and at Bessans – Pont Andagn Fault (Fudral et al., 1998).

The “Medium Susa Valley – Upper Chisone Valley” fault system has a mean direction of N60° and develops in Medium Susa Valley and Upper Chisone Valley. It is characterized by kilometers length structures that displace the preexisting structural and stratigraphic disposition (Giardino and Polino, 1997; Polino et al., 2003). The activity of this system evolved from dextral strike-slip (Oligocene – Miocene) to normal (Malusà, 2004). Col Clapier faults and Venaus faults are related to this system.

Finally, the “Sangone” shear zone has a mean direction of N110° - N120°. It has been identified between Oulx and Bardonecchia and it is characterized by extensional movements (Malusà, 2004).

In Sangone Valley, it corresponds to Sangone shear zone and the kinematic indicators detected in this area show normal and sinistral strike-slip movements.

2.2 La Maddalena tunnel geology

The excavated rock units consist of gneiss and micaschist belonging to the Ambin and Clarea complexes, respectively. In particular, the studied length has been subdivided into three lithologically and mechanically homogeneous domains.

The first one (DI), located from the progressive length (Pk.) 198 m and Pk. 967 m, consists of the gneiss related to Ambin complex. The rock is mainly gray, with greenish coloration in some zones due to the presence of chlorite. The gneiss are characterized by foliated texture, due to the alternation of sialic levels (composed by quartz and feldspars) and lepidoblastic ones (composed of white mica principally). The main orientation of foliation planes registered during tunnel walls mapping is 123°/50° (in terms of dip direction/dip). However, the orientation is not constant throughout the whole domain, due to folding characterized by a mean trend of 325° and a plunge of 60°.

The second homogenous domain (DII), ranging from Pk. 967 to 1360 m, consists in a transition zone between the first and the third homogenous domain, and it consists of an alternation of gneiss and micaschist levels, in variable proportions. From Pk. 1050 m to Pk. 1160 m gneiss is the unique lithology encountered.

The third homogenous domains (DIII) is observed from Pk. 1360 m to Pk. 2010 m and it consists of micaschists, which belong to Clarea complex and are characterized by the alternation of micaceus and sialic layers that define foliation, oriented 116°/31°, that varies in correspondence of folds, following their curvature characterized by an axes orientation of 281°/54°. Quartz percentage is so

variable that, in some zones, the rock is defined as a quartz-micaschist. Within this domain, a cataclastic band was encountered from Pk. 1800 to 2000 m.

In all the investigated tract, schistosity generally dips towards SE, with a medium dip angle (i.e., between 30° and 60°). Metric folds are detected in limited zones only. The most relevant set of fractures, faults and cataclastic zones developed paralleled to the schistosity plains. During the geological surveys, only the fractures showing both evidences of movement (dislocation, kinematic indicators, etc.) and/or cataclastic material filling were considered as faults.

The major shear zones, which are related to the "Sangone shear zone" (Malusà, 2004), were encountered at Pk. 250 m, 800 m, 1130 m, while a cataclastic band was encountered from Pk. 1800 m to 2000 m. A longitudinal geological section of "La Maddalena" tunnel was carried out (Figure 2).

3. Establishment of a database throughout the tunnel

During the excavation of "La Maddalena" tunnel, extensive field work and laboratory tests were performed. A total length of 2010 m, subdivided into 10 m sections, was investigated in order to acquire geological and geotechnical data of rock mass and intact rock properties. The site work included both a detailed tunnel wall mapping of discontinuities and rock coring. The former has allowed to recognize the type of discontinuities (i.e., joints, faults, schistosity planes, veins, etc.), and describing the properties, as orientation, geometry, spacing, weathering and general conditions (following ISRM recommendation, 1978). The rock coring in tunnel wall has allowed to collect samples for laboratory tests, as point load tests, hardness and abrasivity tests, UCS and petrographic analysis. Along the same tract of tunnel TBM data, as boring time, bored lengths and head pressure, have been acquired and registered by a specific acquisition system. In the following

text all rock mass properties and the TBM performance data will be described and statistically analyzed.

3.1 Rock Mass Data

3.1.1 Properties of discontinuities in rock mass

The field survey and mapping allowed describing the types and properties of discontinuities in rock mass as: orientation of fractures and faults, spacing of joints, persistence, roughness, weathering and filling.

More than 1000 orientation data, which were collected in terms of dip direction/dip, were analyzed in order to define the main orientation of each detected set of fractures (Figure 3). The orientation data collected show the same orientations into the three domains, three sets were defined.

The main system, named K1, develops on foliation and it is sub perpendicular to the tunnel axes, the other two sets, less frequents, have a mean dip of 60° and a dip direction N285° and N350° respectively, almost symmetric to tunnel axis.

Besides orientation of discontinuities, also the driven direction of TBM was measured in the field, in order to calculate alpha angle (α), which is the angle between tunnel axis and the planes of weakness. α is generally used for quantifying the influence of discontinuity geometry on TBM performance and can be calculated using the following equation (Bruland, 1998):

$$\alpha = \arcsin(\sin \alpha_f * \sin(\alpha_t - \alpha_s)) \quad (1)$$

where α_f and α_s are respectively dip and strike of encountered planes of discontinuity in rock mass, and α_t is the direction of tunnel axis (in degrees).

It was observed that α, related to the principal set of fractures, is more or less constant over the entire length of tunnel.

Discontinuity surveys have allowed analyzing the distance between weak planes. Scanlines method was adopted. A metallic tape 10m long was fixed on tunnel walls and starting from the tape extreme all intercepted discontinuities were surveyed. For each 10 m length spacing is calculated as the mean distance of consecutive discontinuities. In general, the fractures are more spaced in the gneiss domain (DI) than in remaining parts of tunnel (DII and DIII). In “La Maddalena” tunnel the minimum spacing is 0.30m and the maximum one is 11.80m, a relevant data dispersion was observed. The joint conditions (Jc) were analyzed in terms of persistence, aperture, roughness, infilling and weathering, and were rated according to the fourth parameter of RMR classification system (Bieniawski, 1989).

Regarding the persistence, the modal trace length is included between 3 and 10 m, so that the discontinuities are characterized (in according with IRSM, 1978) by “medium persistence”. Only in few cases, the persistence is “low”. The aperture of joints is generally included between 0.1 mm and 10 mm, than the joints are “closed” or “gapped”.

The roughness of discontinuity surfaces in terms of waviness in the gneiss domain is generally higher than the other sectors of tunnel.

The filling material is mostly absent. In few cases, soft cataclastic material can be found in correspondence of shear zones.

In general, the alteration of discontinuity surfaces is very low and where the discontinuity planes are not fresh, it can be considered slightly weathered. In according to ISRM (1978) the grade of planes alteration is I or II. Also the global weathering grade of rock mass is low.

Resulting Jc ratings are quite constant throughout all tunnel, with ratings ranging from 7 to 29.

The Volumetric Joint Count (Jv; Palmstrom, 1995) is the total number of joints within a unit of volume of rock mass. It is calculated as (Eq. 2):

$$Jv = \sum \left(\frac{1}{S_i}\right) + \left[\frac{N_{r5}}{5}\right] \quad (2)$$

where S_i is the average spacing of the $_i^{th}$ joint set, N_r is the number of random joints along a 5 meters long scanline.

The resulting Jv has high variability within each domain, particularly in DIII. However, DI is characterized by the lowest Jv (i.e., 0-3 joints/m^3).

The groundwater circulation is poor in all investigated tract, only in correspondence of faults and cataclastic zones there are evidences of water circulation. From here the Jw parameter is always high.

3.1.2 Properties of intact rock

UCS is commonly used to assess the rock mass boreability, so that almost all predictive models involve UCS as input parameter, due also to its easy determination. In this study, UCS values were determined by means of point load tests, which were carried out both in site and in laboratory in accordance with ISRM suggested methods (1985). One test every ten excavated m was performed. UCS value was calculated according to the formulation (Eq. 3) proposed by Broch and Franklin (1972):

$$\sigma_c = Is_{50} * 23.7 \quad (3)$$

where Is_{50} is the point load test index corrected to the standard equivalent sample diameter of 50 mm.

UCS decreases from DI (mean value 151 MPa) to DIII (mean value 112.7 MPa).

3.1.3 Mineralogical testing

The quartz content has to be measured into rock masses hosting tunnel construction because it affects abrasivity and hardness of rock, than the Cutter Life Index (CLI).

Several thin sections of excavated rocks were made in order to define the mineralogical phases and evaluate the mineralogical content through petrographic modal analysis. In the studied case, the percentage of quartz decreases from DI to DIII, according to the lithology. DI consists of gneiss, so that the quartz content is around 55-60%. DII, made of alternation of gneiss and micaschist alternation has an average quartz content of 45-50%. Finally, the minimum content, equal to 25-35%, was measured in DIII, which consists of micaschists. These values are in accordance with the results of both mineralogical tests, which made during the tunnel design phase, and the typical values of this kind of rocks.

3.1.4 Rock mass classification systems

The collected data were used to identify the quality class of studied rock masses. In particular, rock mass quality was expressed through RMR (Bieniawski, 1989) and Geological Strength Index (GSI; Hoek, 1994; Hoek et al 1998; Marinos and Hoek, 2000). The RMR, calculated taking into account the adjustment factor for discontinuity orientation, shows that the analyzed rock mass has a general good quality. The resulting RMR values range from 40 to 98. The mean RMR value gently decreases from DI to DII. DI is mostly characterized by very good and good quality classes (I and II RMR classes). Middle and low quality reaches (III, IV RMR classes) are related to fault and cataclastic zones only.

Distribution curve and frequency histogram of geological and mechanical data are shown in Figure 4 and statistical analysis of them is summarized in Table 3.

3.2 TBM field database

During tunnelling all operating parameters were extracted directly from the TBM acquisition system. That allowed their elaboration in order to calculate the useful parameters to be related with rock mass features.

In the last thirty years, many researchers have introduced various TBM performance indexes with the purpose to assess the boreability of rock mass. These include the Penetration Rate (PR or ROP), penetration rate per one cutter-head complete revolution (ROP/rev) or net penetration rate, field penetration index (FPI), specific penetration (SP), which is the inverse of FPI, advance rate (AR) and boreability index (BI). Delisio et al. (2013) introduced FPI for blocky rock conditions (FPI_{blocky}) to estimate TBM performance when di blocky rock conditions are verified.

ROP is defined as the excavated length in a continuous phase during the effective boring time. This time does not include downtimes for TBM maintenance, machine breakdown, excavation stop for support element installation, etc. ROP can be calculated as (Eq.4):

$$ROP = Le/Te \tag{4}$$

where: Le is the excavated length and Te is the effective excavation time. Generally it is expressed in m/h or in mm/min.

Contrariwise, AR is the ratio between excavated distance and total time, which includes the time necessary to drill, installation of supports, TBM ordinary and extra – ordinary maintenance. It can be calculated as (Eq.5):

$$AR = Le/Tt \tag{5}$$

where Le is the excavated length and Tt is the total time necessary to do all tunneling operations. Generally AR is expressed in m/h or in mm/min.

FPI (Nelson et al., 1983) is the ratio between the total force acting on the cutter head or acting on each cutter and the penetration for each complete revolution of TBM head. It represents the force necessary to obtain a determinate penetration during a singular revolution. FPI is measured in kN/cutter/mm/rev or in kN/mm/rev.

In this study ROP and FPI indexes have been utilized.

During this study, about 2200 strokes were analyzed. Generally, TBM performance is lower in DI (i.e., gneiss) than in DII (i.e., gneiss and micaschist alternation) and DIII. (i.e., micaschist only). The highest performance was found in DIII. In other worlds, the ROP increases from DI (where its average value is equal to 0.96 m/h) to DIII (2.18 m/h), while the FPI decreases in the same direction (from 142.73 kN/cutter/mm/rev of DI, to 47.3 kN/cutter/mm/rev of DIII). Distribution curve and frequency histogram of TBM data are shown in Figure 5 and statistical analysis of them is summarized in Table 4.

4. Effect of intact rock/rock mass parameters on TBM performance

TBM performance depends on both intact rock/rock mass properties and operational parameters of the machines.

The TBM parameters considerably changed during the excavation phases, as function of the encountered domain due to the geological and geomechanical features typical of each domain, for this reason the variation of performance trend is not imputable to those parameters that are constant in all studied rock mass. In other worlds TBM performance, for this study, are principally defined by UCS, quartz content, spacing and rock mass quality (expressed by RMR and GSI index). Tunnel depth isn't constant, so the stress levels, however a correlation between tunnel depth and TBM performance hasn't been found.

Uniaxial Compressive Strength

The relation between UCS and TBM performance (ROP and FPI) is shown in Figure 6. In accordance with precedent studies (Farmer and Glassop, 1980; Gong and Zhao, 2009; Graham, 1976; Hamidi et al., 2010; Hughes, 1986), the rock strength is related to TBM performance with an exponential relationship. By increasing the UCS, the ROP decreases and, at the same time, the FPI increases. The empirical equations (Eq. 6-7) relating the UCS and TBM parameters are:

$$ROP = 3.81 * e^{-0.01UCS} \quad (6)$$

$$FPI = 21.55 * e^{0.01*UCS} \quad (7)$$

Quartz content

In the case of "La Maddalena" tunnel the quartz content is estimated from modal analysis on thin section and it is expressed in area percentage. The percentage of quartz seriously affects the TBM performance. In particular, a high content of this mineral reduces the penetration velocity and increases the force necessary to excavations (FPI), by following a linear trend, indirect and direct respectively (Figure 7). Empirical proposed equations are (Eq. 8-9):

$$ROP = -0.035 * q + 2.91 \quad (8)$$

$$FPI = 2.95 * q - 19.05 \quad (9)$$

Distance between weak planes

The correlations between fractures spacing and TBM performances show a parabolic trend (Figure 8). Regarding ROP parameter the minimum values are registered for spacing included between 500 and 1000 cm. In occurrence of low distance between fractures higher values of ROP are measured, due to the better rock mass boreability. Nevertheless, in high fractured rock mass open

TBM gripping is difficult and that determinates a low velocity of penetration because machine force can't be totally used. In high fractured rock mass FPI is lower than FPI in continuous ones. Empirical equations are proposed (Eq. 10-11).

$$ROP = 2E^{-06} * DWP^2 - 0.003 * DWP + 2.07 \quad (10)$$

$$FPI = -0.0002 * DWP^2 + 0.39 * DWP + 33.28 \quad (11)$$

Rock mass quality

Both RMR and GSI were evaluated along a tunnel section 10 m long. Rock mass quality, expressed by RMR and GSI indices, is correlated with TBM measured performance (Figure 9; Figure 10). Quadratic correlations are proposed both for RMR (Eq. 12-13) and GSI (Eq. 14-15):

$$ROP = -0.001 * RMR^2 + 0.09 * RMR - 0.66 \quad (12)$$

$$FPI = 0.05 * RMR^2 - 4.22 * RMR + 137.9 \quad (13)$$

$$ROP = -0.001 * GSI^2 + 0.14 * GSI - 2.49 \quad (14)$$

$$FPI = 0.08 * GSI^2 - 8.07 * GSI + 265.8 \quad (15)$$

By increasing the rock mass quality generally the TBM performance decreases (i.e., the ROP decreases and the FPI increases). However, the TBM performance decrease not only in correspondence of high quality classes, but also in low ones because the weak rock walls cannot contrast the gripper thrust without generating instability of tunnel walls. The top performances are obtained in the good quality class (II), and this is consistent with the findings of previous authors (Sapigni et al., 2002). Nevertheless, the effect of lower classes is not clearly visible for "La Maddalena" tunnel, because of the rock mass has high quality, so that the poor and very poor classes (IV and V) are not represented.

Conclusion

During “La Maddalena” exploratory tunnel (Italy) construction geological, geotechnical and TBM data were collected and analyzed in order to establish the relationship between geological and geotechnical features of rock mass and the performances of TBM. In particular, this study aims to evaluate which rock mass parameters are mostly influencing the realization of underground infrastructures with mechanized methods, for giving to those parameters more attention both during geotechnical site characterization and the preliminary phases of tunnel planning. For this reason a first simplified approach was adopted, at first analysing the variability of the geological-geotechnical rock mass parameter and TBM data along the tunnel, then defining direct empirical correlation between the excavatability indices (ROP and FPI) and each significant rock mass parameter.

The site surveys allowed to subdivide the tunnel in three homogeneous geological domains: the first one (DI) constituted by gneiss formation, the third one (DIII) by micaschist and the second transition domain (DII) with an alternation of gneiss and micaschist levels. The TBM performances are poorest into the gneiss of the first domain and increase into the gneiss/micaschist and micaschist ones, showing a good correspondence with the geological mainly domain.

ROP and FPI have been related to singular rock parameters, in this way easy empirical predictive models about TBM performance were carried out. The site features involved in the analysis were the most variables along the considered tunnel section, the unvaried ones haven’t been considered influencing the TBM behaviour. Tunnel depth (therefore the stress levels) and joint conditions change along the studied portion of tunnel, but there is not a relation between these parameters and machine indices, so they didn’t affect the TBM performances during “La Maddalena” construction. By the comparison between rock properties and TBM indices it has

been noted that UCS, quartz content and the spacing of discontinuities affect the TBM performances more effectively than others geological and geotechnical aspects, so them have to be investigated with greater accuracy. It has been noted that the rock mass quality indices RMR and GSI can be successfully considered to estimate the excavatability of a given material, these results underline the importance of an accurate geological-geotechnical description and characterization of the site hosting the tunnel.

Acknowledgment

The authors would like to thank companies CMC Cooperativa Muratori e Cementisti di Ravenna, Strabag AG and Cogeis SpA for their availability in the machine data collection and geotechnical surveys.

References

Argand, E., Blösch, E., Heim, A., 1911. Les nappes de recouvrement des Alpes pennines et leurs prolongements structuraux, 31-33, In Kommission bei A. Francke (vorm. Schmid & Francke)

Bamford, W.F., 1984. Rock test indices are being successfully correlated with tunnel boring machine performance. In Proceedings of the 5th Australian Tunnelling Conference, Melbourne, 2:9-22

Barton, N., Lien, R., Lunde, J., 1974. Engineering classification of rock masses for the design of tunnel support. Rock Mechanics 6 (4):189-239

Barton, N., 2000. TBM tunnelling in jointed and faulted rock. CRC Press

Bieniawski, Z. T., 1989. Engineering rock mass classifications: a complete manual for engineers and geologists in mining, civil, and petroleum engineering. John Wiley & Sons.

Bilgin, N., Copur, H. and Balci, C., 2013. Mechanical excavation in mining and civil industries. CRC Press.

Blindheim, O.T., 1979. Boreability predictions for tunneling. The Norwegian Institute of Technology, Trondheim, Norway

Brino, G., Peila, D., Steidl, A., Fasching, F., 2015. Prediction of performance and cutter wear in rock TBM: Application to Koralm tunnel project. In: GEAM. GEOINGEGNERIA AMBIENTALE E MINERARIA, vol. 145 n. 2, pp. 37-58. - ISSN 1121-9041

Broch, E., Franklin, J.A., 1972. The point-load strength test. International Journal of Rock Mechanics and Mining Sciences & Geomechanics Abstracts, 9 (6):669-676

Bruland, A., 1998. Hard rock tunnel boring. Doctoral thesis, Norwegian University of Science and Technology, Trondheim, Norway

Casati, C., Giovacchini, A., 1977. L'utilizzo delle immagini Landsat per indagini di neotettonica. Boll. Geod. Sc. Affini, 36:399-410

Crow SC (1975) Jet tunnelling machines. A guide for design. Tunnels & Tunnelling International, 7(2)

Deere, D.U., Hendron, A.J., Patton, F.D., Cording, E.J., 1967. Design of surface and near surface construction in rock. In Failure and breakage of rock, proc. 8th U.S. symp. rock mech., (ed. C. Fairhurst), 237-302. New York: Soc. Min. Engrs, Am. Inst. Min. Metall. Petrolm Engrs.

Delisio, A., & Zhao, J. (2014). A new model for TBM performance prediction in blocky rock conditions. Tunnelling and Underground Space Technology, 43, 440-452.

Desmons, J., Mercier, D., 1993. Passing through the Briançon zone. In Pre-Mesozoic Geology in the Alps, Springer Berlin Heidelberg, pp. 279-295

Dollinger, G.L., Handewith, H.J., Breeds, C.D., 1998. Use of the punch test for estimating TBM performance. Tunnelling and underground space technology, 13(4):403-408

Ellenberger, F., 1958. Etude géologique du pays de Vanoise. Impr. nationale.

Farmer, I.W., Glossop, N.H. 1980. Mechanics of disc cutter penetration. Tunnels and Tunnelling, 12(6):22-25

Fudral, S., 1998. Etude géologique de la suture téthysienne dans les Alpes franco-italiennes nord-occidentales de la Doire Ripaire (Italie) à la région de Bourg-Saint-Maurice(France). Doctoral dissertation

Giardino, M., Polino, R., 1997. Le deformazioni di versante dell'alta valle di Susa: risposta pellicolare dell'evoluzione tettonica recente. Il Quaternario, 10(2):293-298

Gong, Q., Zhao, J., 2009. Development of a rock mass characteristics model for TBM penetration rate prediction. International journal of Rock mechanics and mining sciences, 46(1):8-18

Graham, P.C., 1976. Rock exploration for machine manufacturers. In: Proceedings of the Symposium on Exploration for Rock Engineering, Johannesburg, Balkema, 1:173-180

Grima, M. A., Bruines, P. A., & Verhoef, P. N. W., 2000. Modeling tunnel boring machine performance by neuro-fuzzy methods. Tunnelling and underground space technology, 15(3), 259-269

Hamidi, J.K., Shahriar, K., Rezai, B., Rostami, J., 2010. Performance prediction of hard rock TBM using Rock Mass Rating (RMR) system. Tunnelling and Underground Space Technology, 25(4):333-345

Hassanpour, J., Rostami, J., Zhao, J., 2011. A new hard rock TBM performance prediction model for project planning. Tunnelling and Underground Space Technology, 26(5):595-603

Hassanpour, J., Rostami, J., Khamehchiyan, M., Bruland, A., 2009. Developing new equations for TBM performance prediction in carbonate-argillaceous rocks: a case history of Nowsood water conveyance tunnel. Geomechanics and Geoengineering; an International Journal, 4(4):287-297

Hoek, E., 1994. Strength of rock and rock masses. ISRM News Journal, 2(2):4-16

Hoek, E., Marinos, P., Benissi, M., 1998. Applicability of the Geological Strength Index (GSI) classification for very weak and sheared rock masses. The case of the Athens Schist Formation. Bulletin of Engineering Geology and Environment, 57(2): 151-160

Hughes, H.M., 1986. The relative cuttability of coal-measures stone. Mining Science and Technology, 3(2):95-109

Innaurato, N., Mancini, A., Rondena, E., Zaninetti, A. 1991. Forecasting and effective TBM performances in a rapid excavation of a tunnel in Italy. In proocedings of seventh ISRM Congress, International Society for Rock Mechanics

ISRM, 1985. Suggested method for determining point load strength. International journal of rock mechanics, mining sciences & geomechanics; abstract Vol 22, No 2, pp 51-60.

ISRM, 1978. Suggested methods for the quantitative description of discontinuities in rock masses. International journal of rock mechanics, mining sciences & geomechanics; abstract Vol 15, pp 319-368.

Macias, F. J., Jakobsen, P. D., Seo, Y., & Bruland, A., 2014. Influence of rock mass fracturing on the net penetration rates of hard rock TBMs. Tunnelling and Underground Space Technology, 44, 108-120.

Malusa, M. G., 2004. Post-metamorphic evolution of the Western Alps: kinematic constraints from a multidisciplinary approach (geological mapping, mesostructural analysis, fission-track dating, fluid inclusion analysis).

Marinos, P., Hoek, E., 2000. GSI: a geologically friendly tool for rock mass strength estimation. In Proceedings of ISRM International Symposium, International Society for Rock Mechanics

McFeat-Smith, I., 1999. Mechanised tunnelling for Asia. In Workshop Manual, Organized by IMS Tunnel Consultancy Ltd.

Nelson, P.P., Al-Jalil, Y.A., Laughton, C. 1999. Improved strategies for TBM performance prediction and project management. In Proceedings of the Rapid Excavation and Tunneling Conference, pp. 963-980

Nelson, P. P., Ingraffea, A. R., & O'Rourke, T. D., 1985. TBM performance prediction using rock fracture parameters. In International Journal of Rock Mechanics and Mining Sciences & Geomechanics Abstracts, vol 22(3); 189-192.

Nelson, P.P., O'Rourke, T.D., 1983. Tunnel boring machine performance in sedimentary rocks. Report to Goldberg-Zoino Associates of New York, P.C., School of Civil and Environmental of Civil Engineering. Cornell University, Ithaca, NY, pp. 438

Ozdemir, L., Miller, R.J., Wang, F.D., 1978. Mechanical Tunnel Boring Prediction and Machine Design. NSF APR7307776-A03. Colorado School of Mines. Golden, Colorado, USA

Ozdemir, L., 1977. Development of theoretical equations for predicting tunnel boreability (Doctoral dissertation, Colorado School of Mines).

Palmstrom, A., 1995. RMi-a rock mass characterization system for rock engineering purposes.

Polino, R., De la Pierre, F., Fioraso, G., Giardino, M., Gattiglio, M., 2003 Note illustrative della Carta Geologica d'Italia alla scala 1:50.000, Foglio 132–152–153 Bardonecchia. Servizio Geologico d'Italia, 118

Ramezanzadeh, A., Rostami, J., Tadic, D., 2008. Impact of rock mass characteristics on hard rock TBM performance. 13th Australian tunneling conference, Melbourne, Australia, pp 213–222

Ribacchi, R., Lembo-Fazio, A., 2005. Influence of rock mass parameters on the performance of a TBM in a Gneissic formation (Varzo tunnel). Rock Mech Rock Eng 38(2):105–127

Rostami, J., 1997. Development of a force estimation model for rock fragmentation with disc cutters through theoretical modeling and physical measurement of crushed zone pressure. Doctoral dissertation, Colorado School of Mines

Rostami, J., Ozdemir, L., 1993. A new model for performance prediction of hard rock TBMs. In Proceedings of the Rapid Excavation and Tunneling Conference, pp. 793-793

Roxborough, F.F., Phillips H.R., 1975. Rock excavation by disc cutter. International Journal of Rock Mechanics and Mining Sciences & Geomechanics Abstracts, 12 (12): 361-366

Sanio, H.P., 1985. Prediction of the performance of disc cutters in anisotropic rock. International Journal of Rock Mechanics and Mining Sciences & Geomechanics Abstracts, 22(3):153-161

Sapigni, M., Berti, M., Bethaz, E., Busillo, A., Cardone, G., 2002. TBM performance estimation using rock mass classifications. International Journal of Rock Mechanics and Mining Sciences, 39(6):771-788

Sato, K., Gong, F., & Itakura, K., 1991. Prediction of disc cutter performance using a circular rock cutting ring. In Proceedings 1st international mine mechanization and automation symposium.

Snowdon, R.A., Ryley, M.D., Temporal, J., 1982. A study of disc cutting in selected British rocks. International Journal of Rock Mechanics and Mining Sciences & Geomechanics Abstracts, 19(3):107-121

Spalla, M. I., Zanoni, D., Marotta, A. M., Rebay, G., Roda, M., Zucali, M., & Gosso, G., 2014. The transition from Variscan collision to continental break-up in the Alps: insights from the comparison between natural data and numerical model predictions. Geological Society, London, Special Publications, 405, SP405. 11.

Staub, R., 1937. Gedanken zum bau den Westalpen Zwischen Bernina und Mittelmeer. Buchdruckerei Gebr. Fretz.

Sue, C., Delacou, B., Champagnac, J.D., Allanic, C., Tricart, P., Burkhard, M., 2007. Extensional neotectonics around the bend of the Western/Central Alps: an overview. International Journal of Earth Sciences 96(6):1101-1129

Sundaram, N.M., Rafek, A.G., Komoo, I., 1998. The influence of rock mass properties in the assessment of TBM performance. In Proceedings of the 8th IAEG Congress, Vancouver, British Columbia, Canada, pp. 3553-3559

Sundin, N.O., Wänstedt, S., 1994. A boreability model for TBM's. In proceedings of first North American Rock Mechanics Symposium, American Rock Mechanics Association

Tarkoy, P.J., 1973. Predicting TBM penetration rates in selected rock types. In Proceedings of Ninth Canadian Rock Mechanics Symposium, Montreal

Tarkoy, P. J., 1975. Rock Hardness Index Properties and Geotechnical Parameters for Predicting Tunnel Boring Machine Performance (Doctoral dissertation, University of Illinois at Urbana-Champaign).

Thélin, P., Sartori, M., Lengeler, R., Schaerer, J.P., 1990. Eclogites of Paleozoic or early Alpine age in the basement of the Penninic Siviez-Mischabel nappe, Wallis, Switzerland. Lithos, 25(1):71-88

Wickham, G.E., Tiedemann, H.R., Skinner, E.H., 1972. Support determinations based on geologic predictions. In Proceedings of N Am Rapid Excav & Tunnelling, 1

Wijk, G., 1992. A model of tunnel boring machine performance. Geotechnical and Geological Engineering, 10(1):19-40

Yagiz, S., 2008 Utilizing rock mass properties for predicting TBM performance in hard rock condition. Tunnelling and Underground Space Technology, 23(3):326-339

Yagiz, S., 2006. TBM performance prediction based on rock properties. Proceedings of Multiphysics Coupling and Long Term Behaviour in Rock Mechanics, EUROCK, 6, 663-670.

Yagiz, S., 2002. Development of rock fracture and brittleness indices to quantify the effects of rock mass features and toughness in the CSM Model basic penetration for hard rock tunneling machines. Doctoral dissertation, Colorado School of Mines

Zhao, Z., Gong, Q., Zhang, Y., Zhao, J., 2007. Prediction model of tunnel boring machine performance by ensemble neural networks. Geomechanics and Geoengineering: An International Journal, 2(2):123-128

TABLES

$PR = 5 * Q_{TBM}^{-0.2}$ $Q_{TBM} = \frac{RQD}{J_n} * \frac{J_r}{J_a} * \frac{J_w}{SRF} * \frac{20^9 SIGMA}{F^{10}} * \frac{20}{CLI} * \frac{q}{20} * \frac{\sigma_\theta}{5}$	Barton, 2000
$BI = 37.06 * UCS^{0.26} * Bi^{-0.10} * \left(0.84e^{-0.05Jv} + e^{-0.09*\sin(\alpha+30)}\right)$	Gong and Zhao, 2009
$FPI = 9.401 + 0.397 * Log\alpha + 0.011 * J_c^2 + 1.14E-5 * RDQ^3 + 1.32E-8 * UCS^4$	Hamidi et al., 2010
$FPI = exp(0.008UCS + 0.015RQD + 1.384)$ $ROP = \frac{0.06 * 200 * 7}{FPI}$	Hassanpour et al., 2011
$ROP = 1.093 + 0.029 * PSI - 0.003UCS + 0.437 * Log(\alpha) - 0.219 * DPW$	Yagiz, 2008
$FPI = 0.222BRMR + 2.755$ $FPI = 9.273e^{0.008GSI}$ $FPI = 11.718Q^{0.098}$	Hassanpour et al. 2009
$PR = \sigma_c^{-0.437} - 0.0437RSR + 3.15$	Innaurato et al., 1991
$SP = 250 * \sigma_{cm}^{-0.66}$ $\sigma_{cm} = \sigma_c * exp\left(\frac{RMR - 100}{18}\right)$	Ribacchi and Fazio, 2005
PR = Penetration Rate [m/h]; ROP = Rate of Penetration [m/h]; BI = Boreability Index; CLI = Cutter Life Index; SP = Specific Penetration [m/h]; Q = Rock Tunnelling Quality Index; Q_{TBM} = Q – system classification applied to TBM; RMR =Rock Mass Rating; BRMR = Basic Rock Mass Rating; GSI = Geological Strength Index; RSR = Rock Structure Rating; RQD = Rock Quality Designation [%] (Deere et al., 1967); J_n = Joint Set number; J_r = Joint Roughness number; J_w = Joint Water Reduction factor; J_a = Joint Alteration number; SRF = Stress Reduction Factor; SIGMA = Rock Mass Strength [MPa]; F^{10} = average cutter force [tnf]; q = quartz content [%]; σ_θ = average biaxial stress on tunnel face [MPa]; J_v = total number of joints per m^3 [m^{-3}]; J_c = Rating for Joint conditions; PSI = Peak Slope Index [kN/mm]; DPW = Distance between Planes of Weakness (spacing) [m]; σ_c = rock material uniaxial compressive strength [MPa]; σ_{cm} = rock mass uniaxial compressive strength [MPa]; α = angle between fractures and tunnel axes [deg].	

Table 1. Empirical predictive methods for TBM performances.

machine diameter	6.30 m
cutters diameter	series 17 – 431.8 mm
max recommender individual cutter load	311.5 kN
cutterhead drive	electric motors
max. cutterhead speed	9.3 rpm
main thrust cylinders stroke	1.83 m
N° of main thrust cylinders	4
TBM weight	250 Ton

Table 2. Summary of principal “Gea” parameters.

TUNNEL		DI-GNEISS		DII-MICASCHIST/GNEISS		DIII-MICASCHIST	
UCS [MPa]		UCS [MPa]		UCS [MPa]		UCS [MPa]	
min.	68.0	min.	68.0	min.	70.0	min.	74.0
max.	251.0	max.	219.0	max.	251.0	max.	224.0
mean	133.7	mean	151.0	mean	129.1	mean	112.7
median	129.0	median	143.0	median	129.0	median	105.0
std. dev.	37.6	std. dev.	34.8	std. dev.	39.0	std. dev.	28.3
α [°]		α [°]		α [°]		α [°]	
min.	7.4	min.	18.4	min.	22.5	min.	7.4
max.	85.0	max.	85.0	max.	72.0	max.	69.4
mean	44.8	mean	49.8	mean	40.3	mean	40.7
median	45.2	median	48.3	median	41.6	median	39.8
std. dev.	13.9	std. dev.	12.8	std. dev.	10.8	std. dev.	15.9
Jc		Jc		Jc		Jc	
min.	7.00	min.	11.0	min.	7.0	min.	10.0
max.	29.00	max.	29.0	max.	18.0	max.	21.0
mean	17.94	mean	19.4	mean	15.0	mean	18.0
median	18.00	median	20.0	median	15.0	median	19.0
std. dev.	3.7	std. dev.	4.0	std. dev.	2.5	std. dev.	2.6
DWP [cm]		DWP [cm]		DWP [cm]		DWP [cm]	
min.	27.59	min.	67.9	min.	29.7	min.	30.0
max.	1180.00	max.	1180.0	max.	1000.0	max.	433.3
mean	243.60	mean	356.3	mean	199.7	mean	117.7
median	150.00	median	250.0	median	128.6	median	100.0
std. dev.	234.7	std. dev.	276.7	std. dev.	197.3	std. dev.	62.1
Jv		Jv		Jv		Jv	
min.	0.0	min.	0.0	min.	0.0	min.	1.5
max.	16.0	max.	14.2	max.	14.5	max.	16.0
mean	3.6	mean	1.6	mean	4.0	mean	5.8
median	2.2	median	0.7	median	2.0	median	5.2
std. dev.	3.5	std. dev.	2.6	std. dev.	3.7	std. dev.	3.2
RMR		RMR		RMR		RMR	
min.	40.0	min.	52.0	min.	40.0	min.	44.0
max.	98.0	max.	98.0	max.	86.0	max.	85.0
mean	68.5	mean	75.6	mean	62.3	mean	63.0
median	68.5	median	77.0	median	61.5	median	62.0
std. dev.	12.8	std. dev.	11.1	std. dev.	12.9	std. dev.	9.8
GSI		GSI		GSI		GSI	
min.	43.0	min.	54.0	min.	43.0	min.	48.0
max.	98.0	max.	98.0	max.	84.0	max.	85.0

mean	70.8	mean	77.4	mean	63.9	mean	66.8
median	70.5	median	80.0	median	63.5	median	65.0
std. dev.	11.9	std. dev.	10.2	std. dev.	12.0	std. dev.	9.2

Table 3. Statistical analysis results of geological and geomechanical data.

TUNNEL		DI-GNEISS		DII-MICASCHIST/GNEISS		DIII-MICASCHIST	
ROP [m/h]		ROP [m/h]		ROP [m/h]		ROP [m/h]	
min.	0.3	min.	0.3	min.	0.8	min.	1.1
max.	3.7	max.	2.4	max.	2.6	max.	3.7
mean	1.5	mean	1.0	mean	1.5	mean	2.2
median	1.4	median	0.9	median	1.5	median	2.2
std. dev.	0.7	std. dev.	0.4	std. dev.	0.4	std. dev.	0.5
FPI		FPI		FPI		FPI	
min.	15.2	min.	28.8	min.	33.5	min.	15.2
max.	298.6	max.	298.6	max.	223.0	max.	120.4
mean	1001.0	mean	142.7	mean	94.1	mean	47.3
median	84.8	median	136.3	median	78.5	median	45.5
std. dev.	62.1	std. dev.	57.3	std. dev.	49.3	std. dev.	19.5

Table 4. Statistical analysis results of TBM data.

Table 1. Empirical predictive methods for TBM performances.

Table 2. Summary of principal GEA parameters.

Table 3. Statistical analysis results of geological and geomechanical data.

Table 4. Statistical analysis results of TBM data.

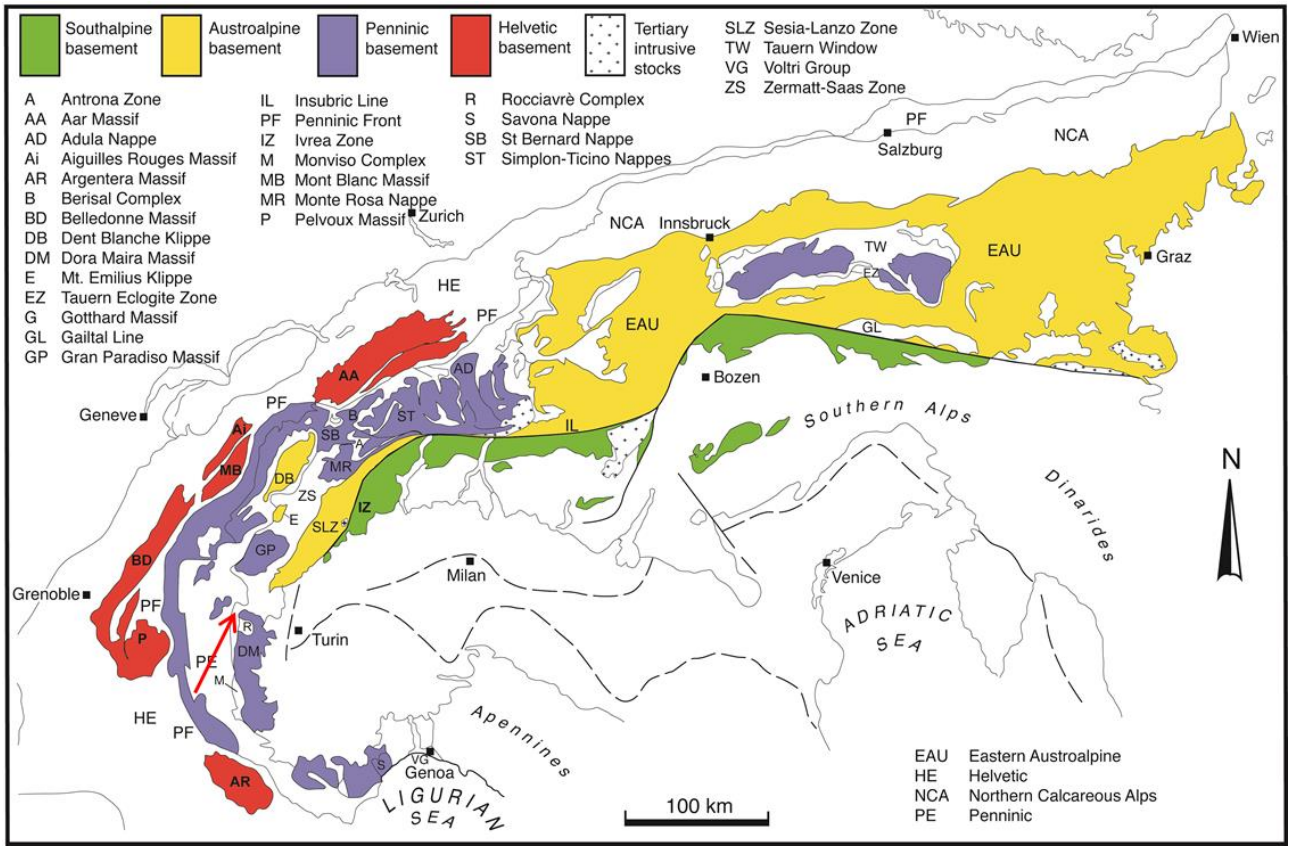

Figure 1. Alpine belt and localization of “La Maddalena” tunnel (red arrow), after Spalla et al. 2014.

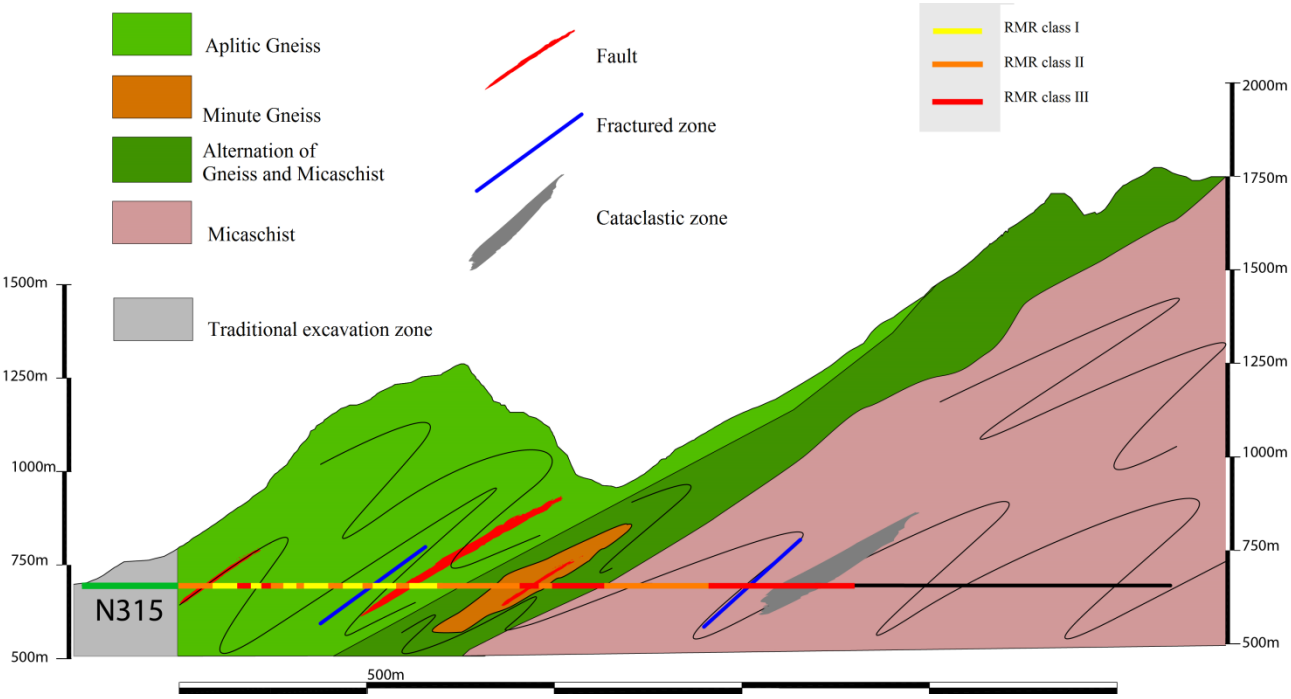

Figure 2. Longitudinal geological section of “La Maddalena” tunnel.

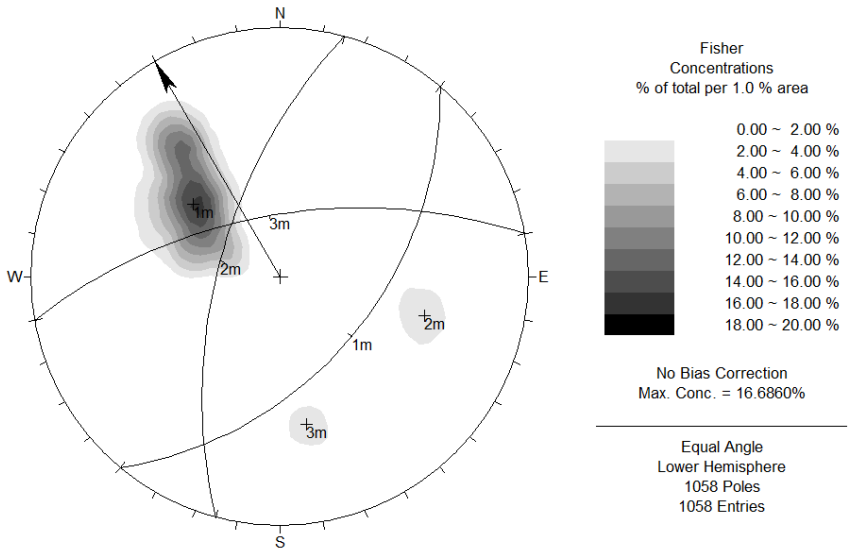

SET ID	Dip direction	Dip
I	130	49
II	285	62
III	350	62

Figure 3. Stereographic projection of discontinuity planes and orientation of principal discontinuity sets.

TUNNEL	DI GNEISS	DII MICASCHIST-GNEISS	DIII MICASCHIST
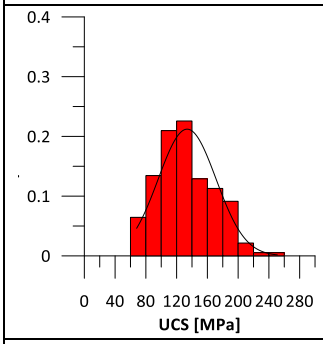	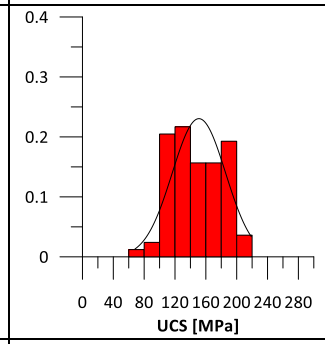	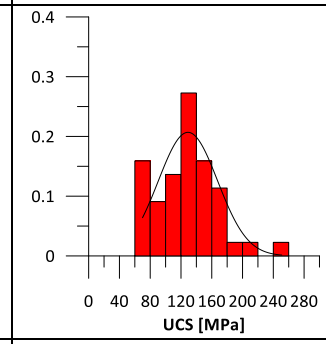	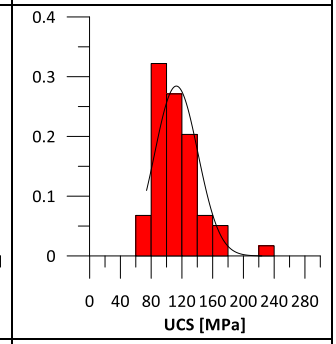
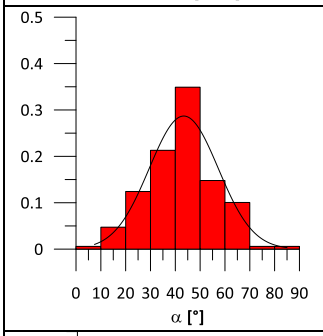	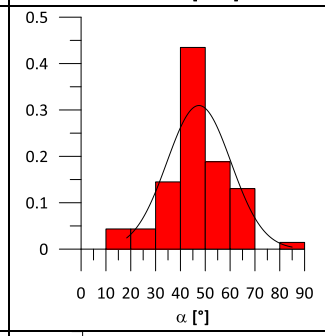	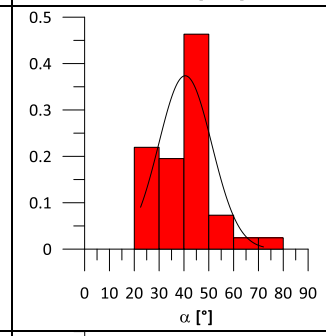	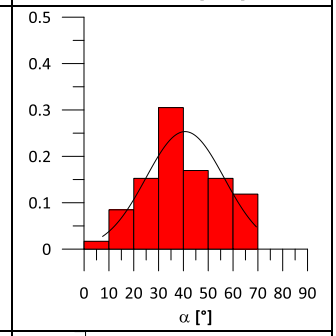
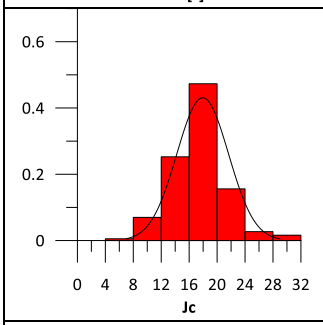	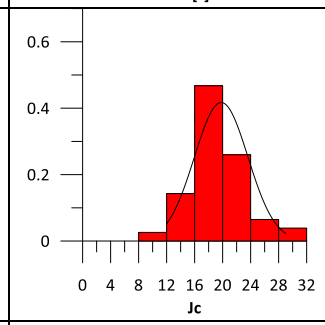	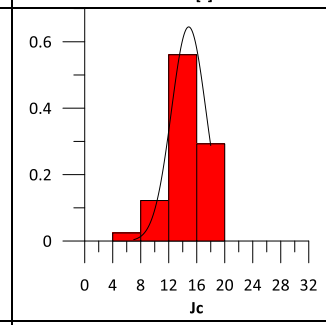	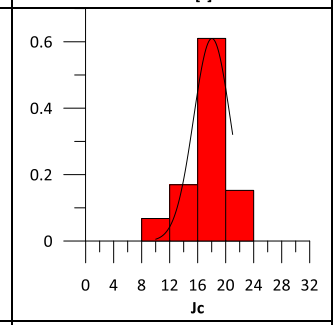
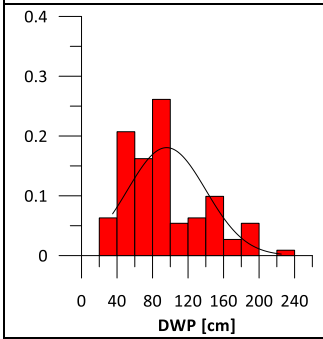	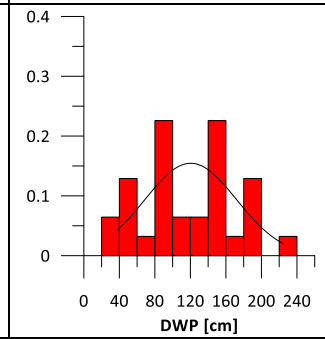	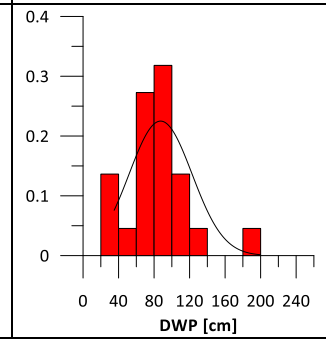	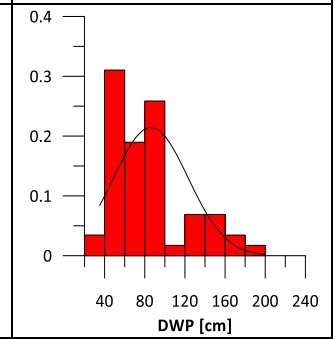
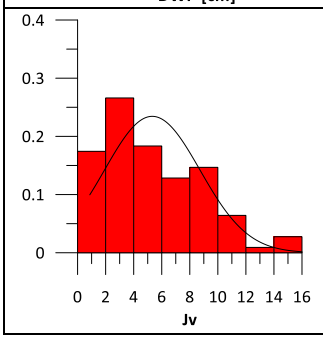	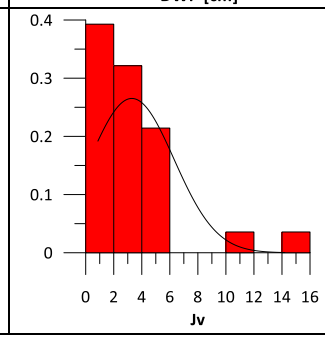	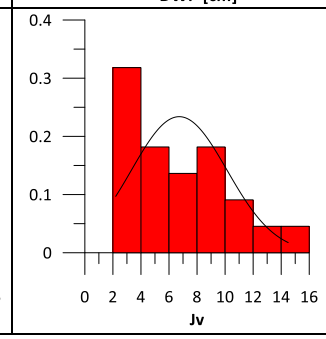	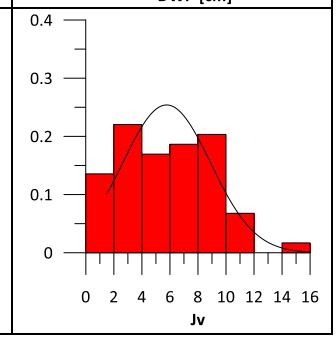

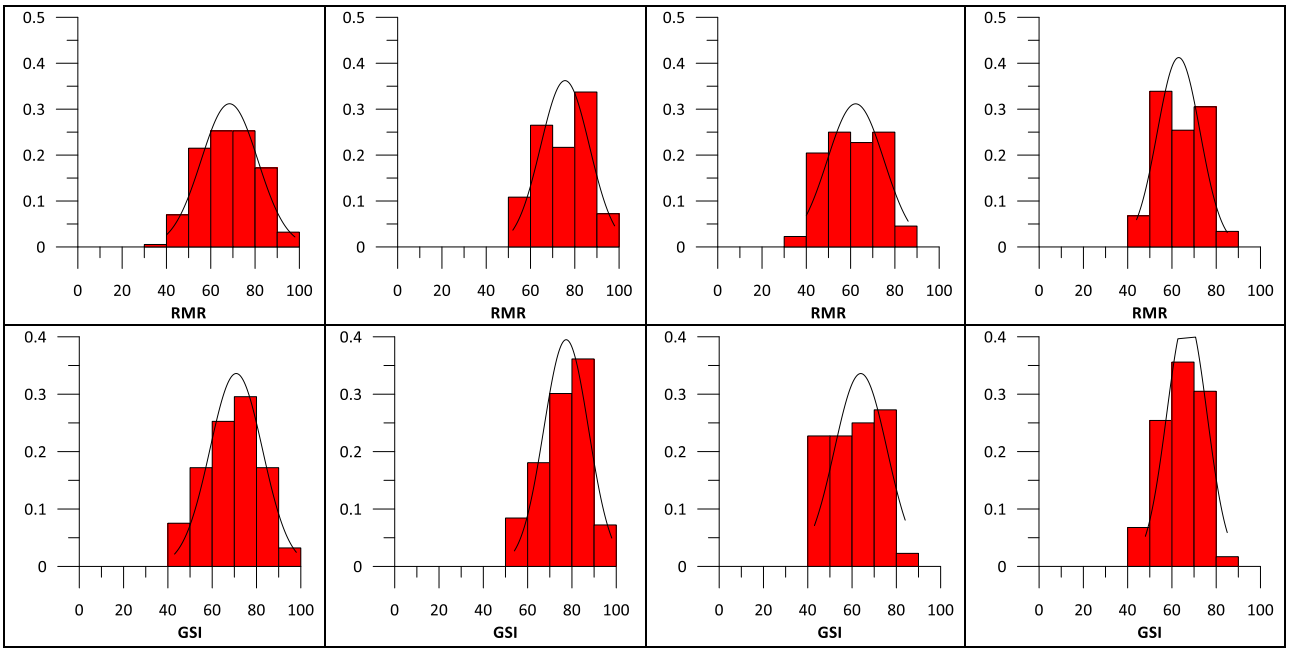

Figure 4. Distribution curve and frequency histogram of geological and geomechanical data.

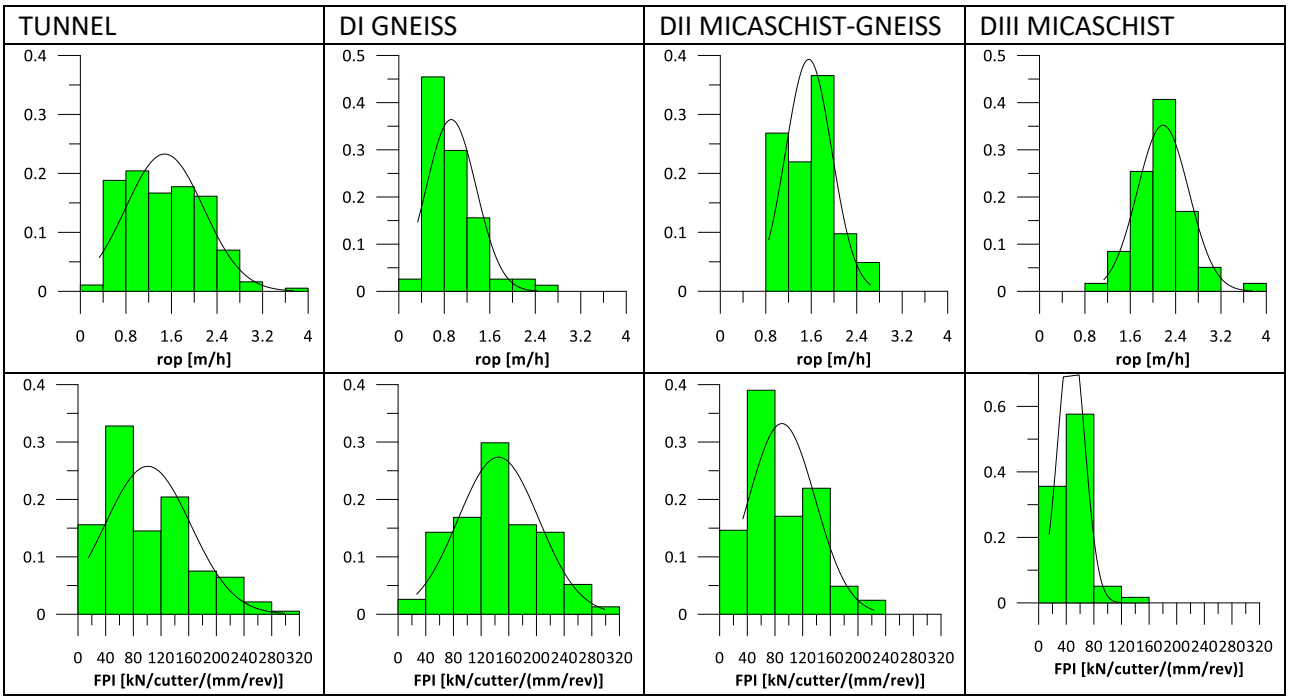

Figure 5. Distribution curve and frequency histogram of TBM data.

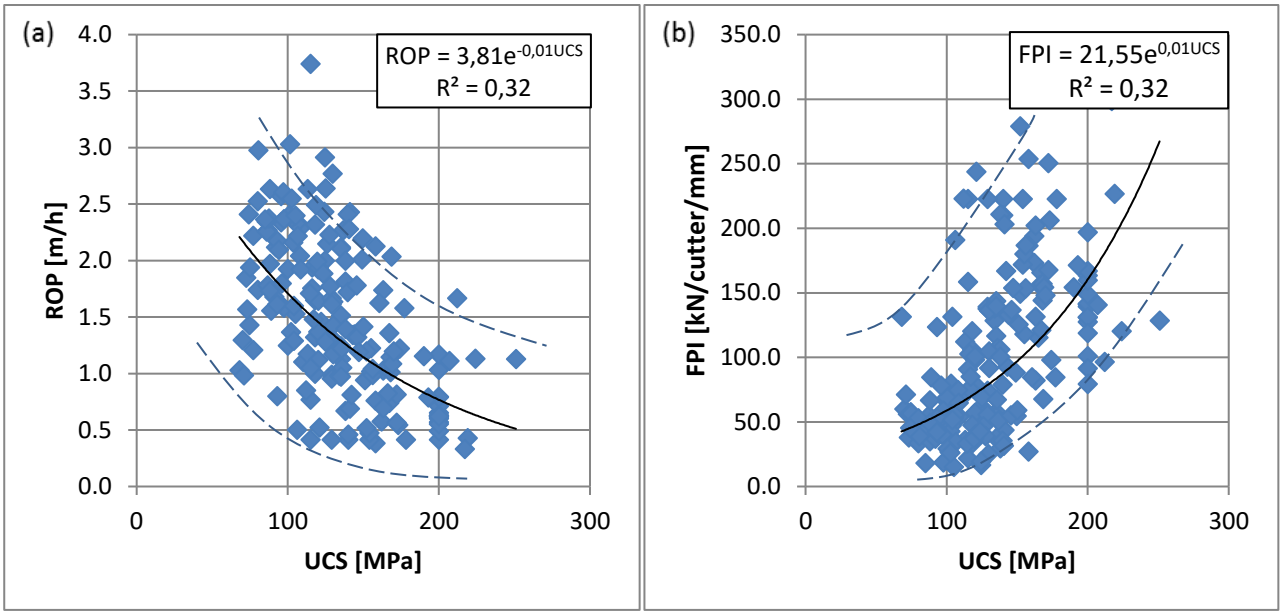

Figure 6. Uniaxial compressive strength vs. ROP (a) and FPI (b) for the all three domains.

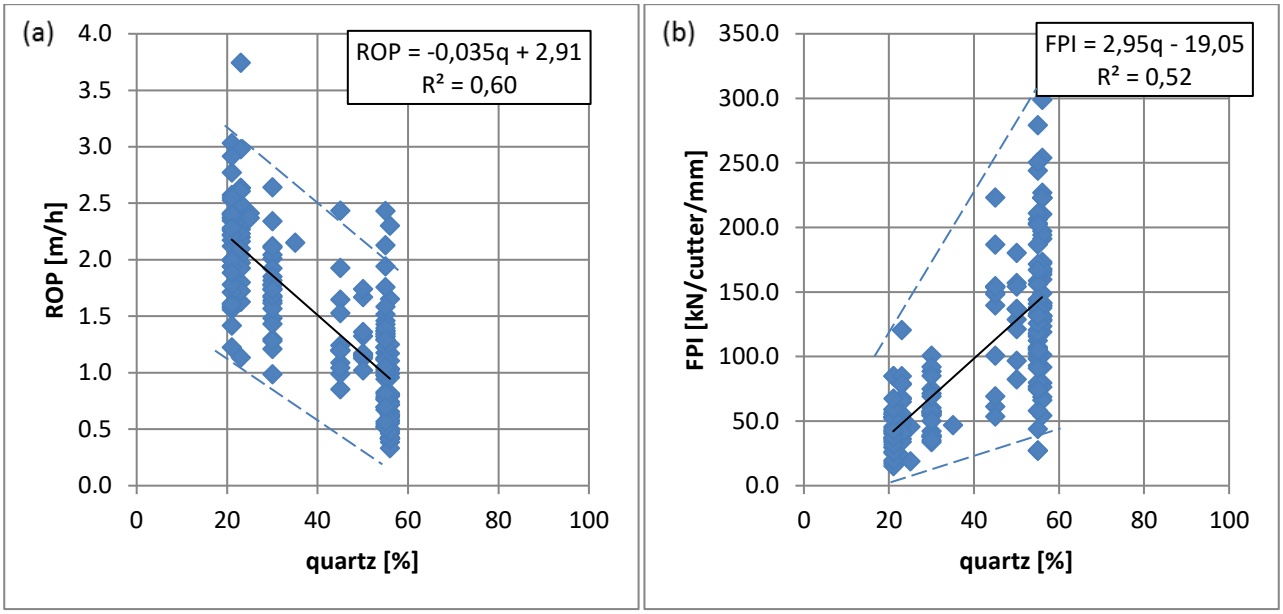

Figure 7. Quartz content vs. ROP (a) and FPI (b) for the all three domains.

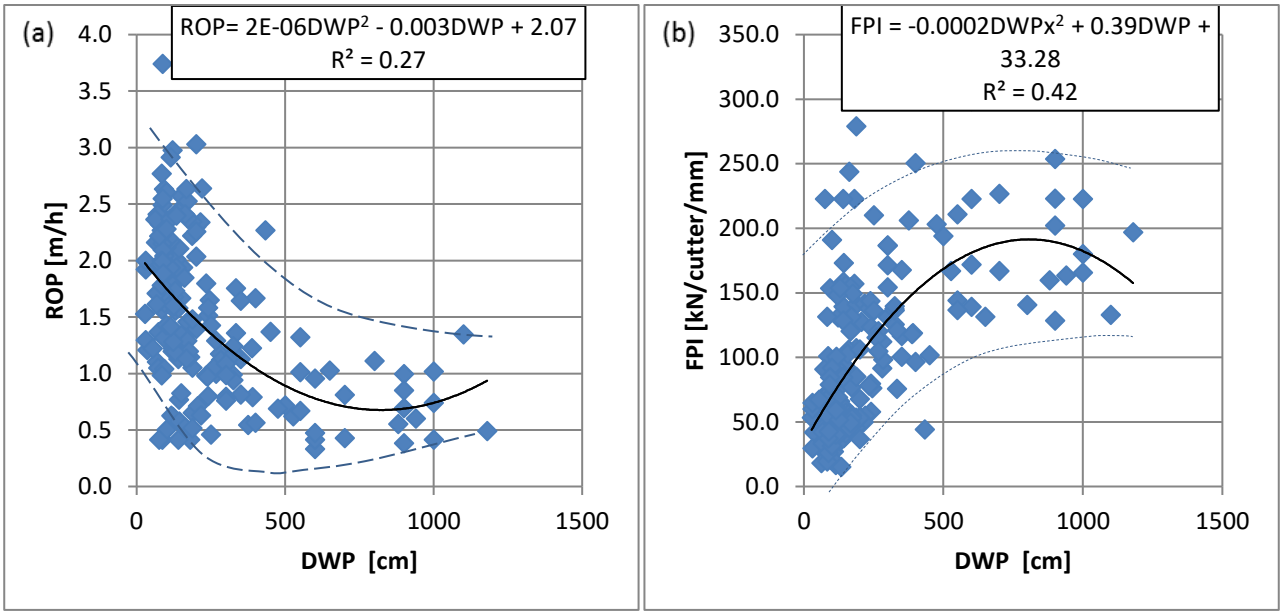

Figure 8. Distance between planes of weakness vs. ROP (a) and FPI (b) for the all three domains.

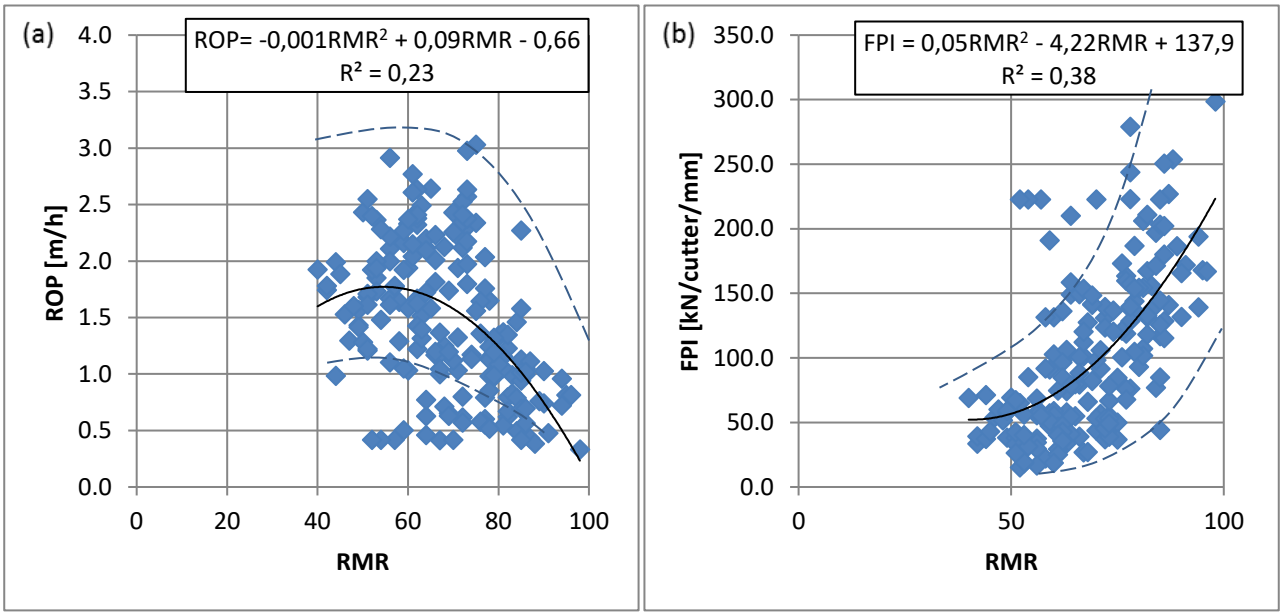

Figure 9. Rock Mass Rating vs. ROP (a) and FPI (b) for the all three domains.

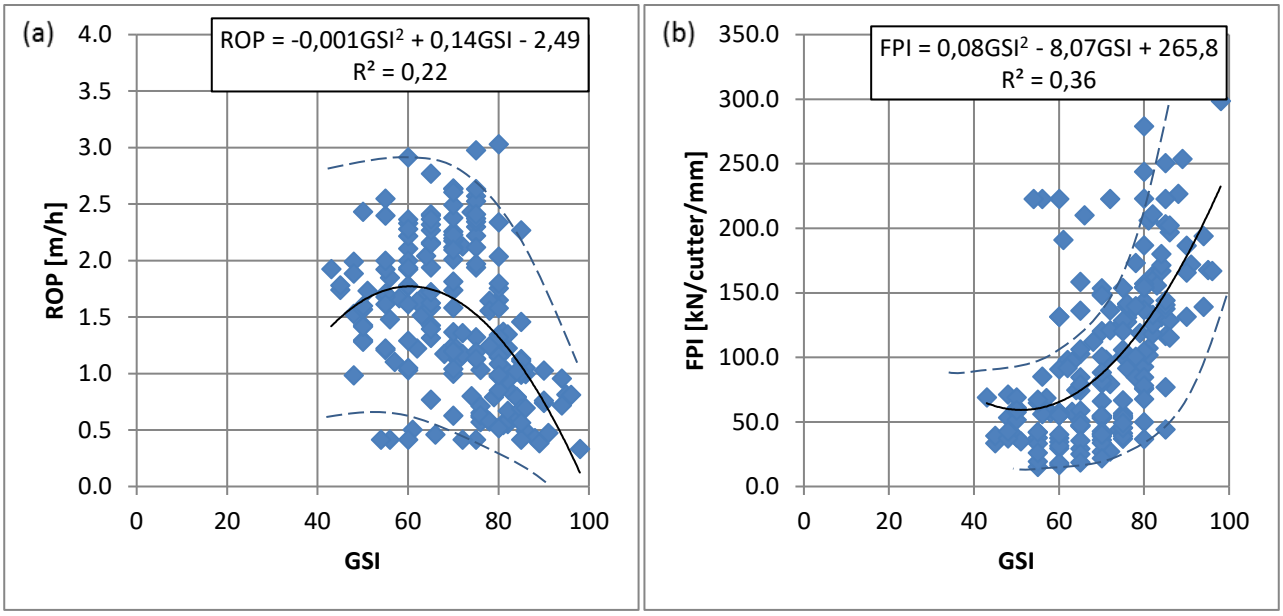

Figure 10. Geological Strength Index vs. ROP (a) and FPI (b) for the all three domains.

FIGURES